

Limitation of Multipoles in BOSS DR12 results

Seokcheon Lee

Research institute of natural science, Gyeongsang national university, jinju 52828, Korea

Recently, the power spectrum (PS) multipoles using the Baryon Oscillation Spectroscopic Survey (BOSS) Data Release 12 (DR12) sample are analyzed [1]. Even though the based model for the analysis is the so-called TNS quasi-linear model including the multipole up to the eighth order in the window function [2], the analysis provides the multipoles up to the hexadecapole. Thus, one might be able to recover the galaxy PS by using the combination of multipoles to investigate the cosmology [3]. We provide the analytic form of this combination of multipoles of the quasi-linear PS including the Fingers of God (FoG) effect to recover the PS at the linear regime. In order to confirm the consistency of the multipole data, we compare the multipole ratios of the linear theory including the FoG effect with those of observation. The data of the ratio of quadrupole to monopole is consistent with that of the linear theory prediction even though the current observational error is too large to distinguish the linear theory prediction from the Kaiser one (*i.e. without the FoG effect*). However, the ratio of hexadecapole to monopole of DR12 is inconsistent with the prediction of the linear theory even at large scale. Thus, the current multipoles data is premature to be used for recovering the galaxy PS.

I. INTRODUCTION

The local concentrations of matter exert a gravitational force on their surroundings, resulting in deviations from the Hubble flow. These are the so-called peculiar velocities of galaxies contaminates the observed redshift, which leads to the difference in the radial position if the redshift is taken as the indicator of the distance. These cause the difference in the spatial clustering between redshift space and real space by producing both squashings and distortions of the spatial distribution of galaxies in the redshift space. These effects are called as the redshift space distortions (RSDs). In the non-linear regime, the random peculiar velocities of galaxies bound in clusters through the virial theorem cause a Doppler shift to make galaxy distribution elongated toward the observer. This is the so-called the Fingers of God (FoG) effect [4, 5]. Thus, the power spectrum parallel to the line of sight (l.o.s.) is suppressed. In the linear regime, the peculiar velocities cause an originally spherical distribution of galaxies to look flattened along the line of sight due to its coherent infall. This is called as the Kaiser effect and enhances the parallel to the l.o.s. component of the power spectrum [6].

The measured quantities are galaxy redshifts and angles from which one transforms our observables redshift into physical coordinates by assuming specific relations between the redshift and the l.o.s. distance and between the angular separation and the distance perpendicular to the line-of-sight given by the fiducial cosmological model. The comoving radial directional distortions depend on the inverse of the Hubble parameter and the angular distortions (*transverse distance direction*) are shown in the angular diameter distance. If the fiducial cosmological model is different from the true cosmology, then it will produce geometric warping and artificially introduce the anisotropic distortions independently from the effect of redshift space distortions. These distortion are called as the Alcock-Paczynski (AP) effects [7]. In addition to RSDs, the AP effects provide the cosmological information from galaxy surveys. These degeneracy on the anisotropy in PS can be broken by using the Baryon Acoustic Oscillations (BAO) feature in the PS [8–10].

The multipole power spectrum analysis is used to measure the growth rate of density per-

turbations, $f = d \ln D_1 / d \ln a$, where D_1 is the growth factor. This gives a simple test of general relativity. The redshift space galaxy PS including both the RSDs and the scaling factors accounting for the AP effects can be modeled as $P_g(f, b, \sigma, \mu, k, z) = \left(\frac{r_s^{\text{fid}}}{r_s}\right)^3 \frac{1}{\alpha_\perp^2 \alpha_\parallel} D_{\text{FoG}}^2(f, \sigma, \mu, k, z) \left(b(k, z) + f(z) \mu^2\right)^2 P_m(k)$, where $\alpha_\parallel = \frac{H^{\text{fid}}(z) r_s^{\text{fid}}(z_d)}{H(z) r_s(z_d)}$, $\alpha_\perp = \frac{D_A(z) r_s^{\text{fid}}(z_d)}{D_A^{\text{fid}}(z) r_s(z_d)}$ with $H^{\text{fid}}(z)$ and $D_A^{\text{fid}}(z)$ are the fiducial values for the Hubble parameter and angular diameter distance at the effective redshifts of the dataset, $r_s^{\text{fid}}(z_d)$ is the fiducial value of the sound horizon scale at the drag epoch assumed in the power spectrum template, μ is the directional cosine between the l.o.s. direction and the wave number vector, $b(k, z)$ is the bias factor, P_m is the mass power spectrum, $D_{\text{FoG}}(k, \mu)$ describes the damping factor due to the FoG effect. The RSDs causes the anisotropy of the clustering amplitude depending on μ . The multipole power spectra are defined by the coefficients of the multipole expansion $P(k, \mu) = \sum_{l=0,2,\dots} P_l(k) \mathcal{L}_l(\mu) (2l+1)$, where $\mathcal{L}_l(\mu)$ are the Legendre polynomials. The monopole P_0 represents the angular averaged power spectrum and is usually what we mean by the power spectrum. $P_2(k)$ is the quadrupole spectrum, which gives the leading anisotropic contribution and can be used to constrain the dark energy [11]. It is also emphasized that combining the monopole and quadrupole power spectra breaks the degeneracies between the multiple bias parameters and dark energy both in the linear and nonlinear regimes.

The anisotropic clustering of the Baryon Oscillation Spectroscopic Survey (BOSS) CMASS both Data Release 11 (DR11) and DR12 have been investigated in Fourier space, using the power spectrum multipoles to measure cosmological parameters [1, 12]. The analysis shows that the low-redshifts ($z_{\text{eff}} = 0.38$ and 0.51) of DR12 constraint is consistent with those of Planck [13]. We show that this statement is correct for the monopole and quadrupole but not for the hexadecapole. Also $k \leq 0.03h/\text{Mpc}$ deviates from the theory. It is known that one can recover the real-space power spectrum from the measurements of the redshift-space multipoles by the same linear combination as in the Kaiser limit [3]. However, if one includes the FoG damping factor, then one needs to generalize the simple Kaiser limit formula. We provide this formula including FoG effect both for the linear theory and the quasi-linear one.

Important point is that one can recover the real space PS from the redshift-space multipoles by using the linear combination of them as in the Kaiser limit. From the real space power spectrum one can obtain the information of the primordial power spectrum like the spectral tilt and the shape parameter. Thus, it is important to check whether the obtained multipoles is accurate enough to extract the real space PS. The ratios of multipoles can be used for this purpose. We use both the Kaiser limit and the Finger of God effect to obtain both the theoretical and observational values of multipole ratios. We obtain the analytic forms of the ratios of the multipoles for both case and compare them with the observational data.

In the next section, we review the ratios of the multipoles for the Kaiser limit linear theory. We also provide the analytic formulae of multipole ratios when one including the FoG effect in the linear theory. We generalize the ratios of the multipoles for the quasi-linear PS in section III. We also provide the analytic formulae of the multipoles using the quasi-linear PS. We compare the observational data with the linear theory prediction to investigate the quality of observed multipoles. We conclude in section IV.

In this section, we review the multipoles of the linear redshift space power spectrum both without and with the FoG factor. We also obtain the analytic forms of multipoles and ratios of them for both cases. The results are independent of linear power spectrum. We use these formulae to obtain the theoretical values of the multipole ratios of the linear theory.

The redshift space position \mathbf{s} of a galaxy differs from its real space position \mathbf{r} due to its peculiar velocity

$$\mathbf{s} = \mathbf{r} + v_z(\mathbf{r})\hat{\mathbf{z}}, \quad (1)$$

where $v_z(\mathbf{r}) \equiv \sigma_z(\mathbf{r})/(aH)$ is the l.o.s component of the galaxy velocity. The galaxy over-density field in redshift space can be obtained by imposing mass conservation, $(1 + \delta_g^s)d^3s = (1 + \delta_g)d^3r$. The exact Jacobian for the real space to redshift space transformation is

$$\frac{(1 + \delta_g)}{(1 + \delta_g^s)} = \frac{d^3r}{d^3s} = \left(1 + \frac{v_z}{z}\right)^2 \left(1 + \frac{dv_z}{dz}\right). \quad (2)$$

In the limit where we are looking at scales much smaller than the mean distance to the pair, $v_z/z \ll 1$ and then it is only the second term that is important

$$(1 + \delta_g^s) = (1 + \delta_g) \frac{d^3r}{d^3s} \simeq (1 + \delta_g) \left(1 + \frac{dv_z}{dz}\right)^{-1}. \quad (3)$$

If we assume an irrotational velocity field, then we can write $v_z = -\partial/\partial z \nabla^{-2}\theta$, where $\theta = -\nabla \cdot \mathbf{v}$. In the Fourier space, $(\partial/\partial z)^2 \nabla^{-2} = (k_z/k)^2 = \mu^2$ where μ is the cosine of the angle between the wave vector, k and the l.o.s. Thus, Eq.(3) becomes

$$\delta_g^s(k) = \delta_g(k) + \mu^2\theta(k), \quad (4)$$

to the linear order. Often it is further assumed that the velocity field comes from the linear perturbation theory of the matter

$$\theta(k) = f\delta_m(k), \quad (5)$$

where $f \equiv d \ln D_1 / d \ln a$ is the growth index with D_1 is the growth factor. On large scales, the galaxies along the l.o.s appear closer to each other than their actual distance because mass flows from low-density regions onto high density sheets (Kaiser effect) [6]. If we relate the galaxy density perturbation with the matter density one as $\delta_g = b(z, k)\delta_m$ with b being the so-called bias factor. In the Kaiser limit, the linear redshift space galaxy power spectrum is given by [14]

$$P_g(f, b, \mu, k, z) = \left(b(k, z) + f(z)\mu^2\right)^2 P_{\delta\delta}(k, z) \simeq b(z)^2 \left(1 + \beta(z)\mu^2\right)^2 P_{\delta\delta}(k, z), \quad (6)$$

where $P_{\delta\delta}$ is the linear matter power spectrum obtained from the line theory and we use the assumption that the bias factor is scale independent at the linear regime in the second equality. From the above Eq. (6), the Kaiser limit linear theory multipoles are given by

$$P_0^{\text{Kai}} = \frac{b^2}{15} (15 + 10\beta + 3\beta^2) P_{\delta\delta} = \frac{b^2}{15} \left(15 + 10\frac{f}{b} + 3\frac{f^2}{b^2}\right) P_{\delta\delta}, \quad (7)$$

$$P_2^{\text{Kai}} = \frac{4}{21} b^2 \beta (7 + 3\beta) P_{\delta\delta} = \frac{4}{21} f (7b + 3f) P_{\delta\delta}, \quad (8)$$

$$P_4^{\text{Kai}} = \frac{8}{35} b^2 \beta^2 P_{\delta\delta} = \frac{8}{35} f^2 P_{\delta\delta}. \quad (9)$$

The ratios of these multipoles are well known as

4

$$R_2^{\text{Kai}} \equiv \frac{P_2^{\text{Kai}}}{P_0^{\text{Kai}}} = \frac{20\beta(7+3\beta)}{7(15+10\beta+3\beta^2)} = \frac{20f(7b+3f)}{7(15b^2+10bf+3f^2)}, \quad (10)$$

$$R_4^{\text{Kai}} \equiv \frac{P_4^{\text{Kai}}}{P_0^{\text{Kai}}} = \frac{24\beta^2}{7(15+10\beta+3\beta^2)} = \frac{24f^2}{7(15b^2+10bf+3f^2)}. \quad (11)$$

These ratios of multipoles are independent of the linear power spectrum, $P_{\delta\delta}$ and thus one can obtain the growth index, f and the bias factor, b from observed values of multipoles. The linear matter PS is recovered by using the linear combination of multipoles

$$P_{\delta\delta} = \frac{1}{b^2} \left(P_0^{\text{Kai}} - \frac{1}{2} P_2^{\text{Kai}} + \frac{3}{8} P_4^{\text{Kai}} \right). \quad (12)$$

One can extend the above consideration including the FoG effect. Then the linear redshift space power spectrum is given by

$$P_g(f, b, \sigma, \mu, k, z) \rightarrow D_{\text{FoG}}^2(f, \sigma, \mu, k, z) b(z)^2 \left(1 + \beta(z) \mu^2 \right)^2 P_{\delta\delta}(k, z), \quad (13)$$

where the FoG factor can be chosen as either the Gaussian or the Lorentzian [3, 15, 16]

$$D_{\text{FoG}}^{\text{Gau}}(f, \sigma, \mu, k, z) = \exp \left[-\frac{\sigma^2(z) f^2(z) k^2 \mu^2}{2H^2(z)} \right], \quad (14)$$

$$D_{\text{FoG}}^{\text{Lor}}(k, z, \sigma, \mu) = \left(1 + \frac{\sigma^2(z) f^2(z) k^2 \mu^2}{H^2(z)} \right)^{-1/2}, \quad (15)$$

$$D_{\text{FoG}}^{\text{Lorh}}(k, z, \sigma, \mu) = \left(1 + \frac{\sigma^2(z) f^2(z) k^2 \mu^2}{2H^2(z)} \right)^{-1/2}, \quad (16)$$

where we also introduce the so-called ‘‘dispersion model’’ for the Lorentzian model given in [3]. We replace the term inside of the function as

$$\frac{x}{k} \equiv \frac{\sigma(z) f(z)}{H(z)} = \frac{\sigma_0}{D_0 H_0} \frac{D(z) f(z)}{E(z)} = \frac{\sigma_0 f_0}{H_0} \frac{D'(z)}{D'(z_0)} \frac{(1+z)}{E(z)}, \quad (17)$$

where $\sigma(z) = \frac{D(z)}{D_0} \sigma_0$, $f(z) = \frac{a}{D(a)} \frac{dD}{da} = -\frac{(1+z)}{D(z)} D'(z)$, $D'(z) \equiv \frac{dD(z)}{dz}$, and $E(z) \equiv \frac{H(z)}{H_0} = \sqrt{\Omega_{m0}(1+z)^3 + (1-\Omega_{m0})(1+z)^{3(1+\omega_0)}}$. We assume the flat ω CDM model with the constant dark energy equation of state, ω_0 in $E(z)$.

The multipoles with the Gaussian FoG factor of Eq. (14) are given by

$$P_0^{\text{lin}} = -\frac{e^{-x^2} (6f^2x + 4f(2b+f)x^3 - e^{x^2} \sqrt{\pi} (3f^2 + 4bfx^2 + 4b^2x^4) \text{Erf}[x]) P_{\delta\delta}}{8x^5}, \quad (18)$$

$$P_2^{\text{lin}} = -\frac{5e^{-x^2} (12b^2x^4 + 4bfx^2(9+4x^2) + f^2(45+24x^2+8x^4)) P_{\delta\delta}}{16x^6} + \frac{5\sqrt{\pi} (45f^2 + 6(6b-f)fx^2 + 4b(3b-2f)x^4 - 8b^2x^6) \text{Erf}[x] P_{\delta\delta}}{32x^7}, \quad (19)$$

$$P_4^{\text{lin}} = -\frac{9e^{-x^2} (20b^2x^4(21+2x^2) + 4bfx^2(525+170x^2+32x^4) + f^2(3675+1550x^2+416x^4+64x^6)) P_{\delta\delta}}{128x^8} + \frac{27\sqrt{\pi} (4bfx^2(175-60x^2+4x^4) + 4b^2x^4(35-20x^2+4x^4) + f^2(1225-300x^2+12x^4)) \text{Erf}[x] P_{\delta\delta}}{256x^9}, \quad (20)$$

where Erf defines the error function. Thus, the ratios of multipoles are given by

$$\begin{aligned} R_2^{\text{lin}} &\equiv \frac{P_2^{\text{lin}}}{P_0^{\text{lin}}} = \frac{5 \left(90f^2x + 24f(3b+2f)x^3 + 8(3b^2+4bf+2f^2)x^5 \right)}{4x^2 \left(6f^2x + 4f(2b+f)x^3 - e^{x^2} \sqrt{\pi} (3f^2 + 4bfx^2 + 4b^2x^4) \text{Erf}[x] \right)} \\ &- \frac{5e^{x^2} \sqrt{\pi} \left(45f^2 + 6f(6b-f)x^2 + 4b(3b-2f)x^4 - 8b^2x^6 \right) \text{Erf}[x]}{4x^2 \left(6f^2x + 4f(2b+f)x^3 - e^{x^2} \sqrt{\pi} (3f^2 + 4bfx^2 + 4b^2x^4) \text{Erf}[x] \right)}, \end{aligned} \quad (21)$$

$$\begin{aligned} R_4^{\text{lin}} &\equiv \frac{P_4^{\text{lin}}}{P_0^{\text{lin}}} = \frac{9 \left(20b^2x^5(21+2x^2) + 4bfx^3(525+170x^2+32x^4) + f^2x(3675+1550x^2+416x^4+64x^6) \right)}{16x^4 \left(6f^2x + 4f(2b+f)x^3 - e^{x^2} \sqrt{\pi} (3f^2 + 4bfx^2 + 4b^2x^4) \text{Erf}[x] \right)} \\ &- \frac{27e^{x^2} \sqrt{\pi} \left(4bfx^2(175-60x^2+4x^4) + 4b^2x^4(35-20x^2+4x^4) + f^2(1225-300x^2+12x^4) \right) \text{Erf}[x]}{32x^4 \left(6f^2x + 4f(2b+f)x^3 - e^{x^2} \sqrt{\pi} (3f^2 + 4bfx^2 + 4b^2x^4) \text{Erf}[x] \right)}. \end{aligned} \quad (22)$$

As expected, all of these forms Eqs.(18)-(22) are independent of the linear matter power spectrum as in the Kaiser limit. Also, these results are equal to those of the Kaiser limit given by Eqs.(7)-(11) when one adopts $x \rightarrow 0$ limit in the above Eqs.(18)-(22). We show the multipoles and their ratios for the Lorentzian FoG factors of Eqs.(15) and (16) in the Appendix. As in the Kaiser limit case, one can obtain the linear power spectrum, $P_{\delta\delta}$ from the linear combinations of the multipoles

$$P_{\delta\delta} = P_0^{\text{lin}} + c_2^{\text{lin}} P_2^{\text{lin}} + c_4^{\text{lin}} P_4^{\text{lin}}, \quad (23)$$

$$c_4^{\text{lin}} = \frac{- \left(16x^3 \left(4x^2 \left(4bfx^2 + 4e^{x^2}x^4 + f^2(3+2x^2) \right) + 5c_2^{\text{lin}} \left(12b^2x^4 + 4bfx^2(9+4x^2) + f^2(45+24x^2+8x^4) \right) \right) \right)}{c_2^{\text{lin}}} \quad (24)$$

$$- \frac{\left(8e^{x^2} \sqrt{\pi} x^2 \left(-4(3f^2x^2 + 4bfx^4 + 4b^2x^6) + 5c_2^{\text{lin}} \left(4bfx^2(-9+2x^2) + 4b^2x^4(-3+2x^2) + f^2(-45+6x^2) \right) \right) \text{Erf}[x] \right)}{c_2^{\text{lin}}},$$

$$\begin{aligned} c_2^{\text{lin}} &= 18x(20b^2x^4(21+2x^2) + 4bfx^2(525+170x^2+32x^4) + f^2(3675+1550x^2+416x^4+64x^6)) \\ &- 27e^{x^2} \sqrt{\pi} \left(4bfx^2(175-60x^2+4x^4) + 4b^2x^4(35-20x^2+4x^4) + f^2(1225-300x^2+12x^4) \right) \text{Erf}[x]. \end{aligned} \quad (25)$$

The above Eq.(23) is the extended version of Eq.(12) when one includes the FoG effect in the multipoles.

One can extend the linear matter power spectrum to the quasi-linear one by using the standard perturbation theory. If one approximate the redshift space power spectrum up to only $l = 0, 2, 4$ multipoles, one can always write [3, 17]

$$P_s(k) = P(k) \left[1 + 2A_2(k)\mu^2 + A_4(k)\mu^4 \right], \quad (26)$$

where A_2 and A_4 are some arbitrary functions of k . It is shown that one can recover the matter power spectrum by using the same linear combination as in the Kaiser limit if the FoG effect is not included [3]. This statement can be extended to the multipoles including the FoG effect as shown in Eq.(23). This is proper because the multipoles higher than $l = 4$ are generated only for $k \geq 0.2h/\text{Mpc}$. In the next section, we investigate the above results with DR 12 data [1].

III. QUASI-LINEAR SCALE

DR12 uses the TNS model for the anisotropic galaxy power spectrum in their analysis [2]

$$\begin{aligned} P_g^{\text{(TNS)}}(k, \mu) &= \exp \left(-fk\mu\sigma_v \right)^2 \left[P_{g,\delta\delta}(k) + 2f\mu^2 P_{g,\delta\theta}(k) + f^2\mu^4 P_{\theta\theta}(k) + b_1^3 A(k, \mu, \beta) + b_1^4 B(k, \mu, \beta) \right] \\ &\equiv \exp \left(-fk\mu\sigma_v \right)^2 \left[P_{g,\delta\delta}(k) + \mu^2 \mathcal{A}(k) + \mu^4 \mathcal{B}(k) + \mu^6 \mathcal{C}(k) + \mu^8 \mathcal{D}(k) \right] \end{aligned} \quad (27)$$

$$\simeq \exp \left(-fk\mu\sigma_v \right)^2 \left[P_{g,\delta\delta}(k) + \mu^2 \mathcal{A}(k) + \mu^4 \mathcal{B}(k) \right] \quad (28)$$

$$A(k, \mu, b) = (k\mu f) \int \frac{d^3q}{(2\pi)^3} \frac{q_z}{q^2} \left[B_\sigma(\vec{q}, \vec{k} - \vec{q}, -\vec{k}) - B_\sigma(\vec{q}, \vec{k}, -\vec{k} - \vec{q}) \right], \quad (29)$$

$$B(k, \mu, b) = (k\mu f)^2 \int \frac{d^3q}{(2\pi)^3} F(\vec{q}) F(\vec{k} - \vec{q}), \quad (30)$$

$$(2\pi)^3 \delta_D(\vec{k}_{123}) B_\sigma(\vec{k}_1, \vec{k}_2, \vec{k}_3) \equiv \left\langle \theta(\vec{k}_1) \left[b(k_2) \delta(\vec{k}_2) + f \frac{k_{2z}^2}{k_2^2} \theta(\vec{k}_2) \right] \left[b(k_3) \delta(\vec{k}_3) + f \frac{k_{3z}^2}{k_3^2} \theta(\vec{k}_3) \right] \right\rangle, \quad (31)$$

$$F(\vec{q}) \equiv \frac{q_z}{q^2} \left[b(q) P_{\delta\theta}(q) + f \frac{q_z^2}{q^2} P_{\theta\theta}(q) \right]. \quad (32)$$

In order to obtain the ratios of multipoles up to hexadecapole, one needs to consider the terms up to μ^4 in the above Eq.(27) and thus we use the approximation of it given by Eq.(28). This approximation is also used in the data analysis except including the window function up to $l = 8$ [1]. It has been shown that the recovering the real-space power spectrum from the redshift-space multipoles is still given by the same linear combination as in the Kaiser limit up to $k < 0.2 h\text{Mpc}^{-1}$ and this fact rationalizes this approximation [3, 18, 19].

From the above Eq.(28), one obtain the multipoles

$$P_0^{\text{Quas}} = \frac{-e^{-x^2} (3\mathcal{B} + 2(\mathcal{A} + \mathcal{B})x^2)}{4x^4} + \frac{\sqrt{\pi} \text{Erf}[x] (3\mathcal{B} + 2\mathcal{A}x^2 + 4x^4 P_{g,\delta\delta})}{8x^5}, \quad (33)$$

$$P_2^{\text{Quas}} = \frac{-5e^{-x^2} (45\mathcal{B} + 6(3\mathcal{A} + 4\mathcal{B})x^2 + 8(\mathcal{A} + \mathcal{B})x^4 + 12x^4 P_{g,\delta\delta})}{16x^6} + \frac{5\sqrt{\pi} \text{Erf}[x] (45\mathcal{B} + 6(3\mathcal{A} - \mathcal{B})x^2 - 4\mathcal{A}x^4 + 4x^4 (3 - 2x^2) P_{g,\delta\delta})}{32x^7}, \quad (34)$$

$$P_4^{\text{Quas}} = \frac{-9e^{-x^2} (3675\mathcal{B} + 50(21\mathcal{A} + 31\mathcal{B})x^2 + 4(85\mathcal{A} + 104\mathcal{B})x^4 + 64(\mathcal{A} + \mathcal{B})x^6 + 20x^4 (21 + 2x^2) P_{g,\delta\delta})}{128x^8} + \frac{27\sqrt{\pi} \text{Erf}[x] (1225\mathcal{B} + 50(7\mathcal{A} - 6\mathcal{B})x^2 - 12(10\mathcal{A} - \mathcal{B})x^4 + 8\mathcal{A}x^6 + 4x^4 (35 - 4x^2 (5 - x^2)) P_{g,\delta\delta})}{256x^9}. \quad (35)$$

From these Eqs.(33)-(35), the ratios of the multipoles are given by

$$R_2^{\text{Quas}} = \frac{5(45\mathcal{B} + 6(3\mathcal{A} + 4\mathcal{B})x^2 + 8(\mathcal{A} + \mathcal{B})x^4 + 12x^4 P_{g,\delta\delta})}{2x(6\mathcal{B}x + 4(\mathcal{A} + \mathcal{B})x^3 - e^{x^2} \sqrt{\pi} \text{Erf}[x] (3\mathcal{B} + 2\mathcal{A}x^2 + 4x^4 P_{g,\delta\delta}))} + \frac{5e^{x^2} \sqrt{\pi} \text{Erf}[x] (-45\mathcal{B} - 6(3\mathcal{A} - \mathcal{B})x^2 + 4\mathcal{A}x^4 - 4x^4 (3 - 2x^2) P_{g,\delta\delta})}{4x^2(6\mathcal{B}x + 4(\mathcal{A} + \mathcal{B})x^3 - e^{x^2} \sqrt{\pi} \text{Erf}[x] (3\mathcal{B} + 2\mathcal{A}x^2 + 4x^4 P_{g,\delta\delta}))}, \quad (36)$$

$$R_4^{\text{Quas}} = \frac{9(3675\mathcal{B} + 50(21\mathcal{A} + 31\mathcal{B})x^2 + 4(85\mathcal{A} + 104\mathcal{B})x^4 + 64(\mathcal{A} + \mathcal{B})x^6 + 20x^4 (21 + 2x^2) P_{g,\delta\delta})}{16x^3(6\mathcal{B}x + 4(\mathcal{A} + \mathcal{B})x^3 - e^{x^2} \sqrt{\pi} \text{Erf}[x] (3\mathcal{B} + 2\mathcal{A}x^2 + 4x^4 P_{g,\delta\delta}))} - \frac{27e^{x^2} \sqrt{\pi} \text{Erf}[x] (1225\mathcal{B} + 50(7\mathcal{A} - 6\mathcal{B})x^2 - 12(10\mathcal{A} - \mathcal{B})x^4 + 8\mathcal{A}x^6 + 4x^4 (35 - 4x^2 (5 - x^2)) P_{g,\delta\delta})}{32x^4(6\mathcal{B}x + 4(\mathcal{A} + \mathcal{B})x^3 - e^{x^2} \sqrt{\pi} \text{Erf}[x] (3\mathcal{B} + 2\mathcal{A}x^2 + 4x^4 P_{g,\delta\delta}))}. \quad (37)$$

One can extract $P_{g,\delta\delta}$, \mathcal{A} , and \mathcal{B} from observed multipoles values by using the above Eqs.(33)-(35),

$$P_{g,\delta\delta} = \frac{N_{P_{\delta\delta}P_0} + N_{P_{\delta\delta}P_2} + N_{P_{\delta\delta}P_4}}{D_P}, \quad (38)$$

$$\mathcal{A} = \frac{N_{\mathcal{A}P_0} + N_{\mathcal{A}P_2} + N_{\mathcal{A}P_4}}{D_P}, \quad (39)$$

$$\mathcal{B} = \frac{N_{\mathcal{B}P_0} + N_{\mathcal{B}P_2} + N_{\mathcal{B}P_4}}{D_P}, \quad (40)$$

$$\begin{aligned} N_{P_{\delta\delta}P_0} &= 21e^{x^2}x \left(4x^2(675 + 600x^2 + 16x^4 + 8x^6) + 4e^{x^2}\sqrt{\pi}x(-675 - 150x^2 + 124x^4 - 44x^6 + 8x^8)\text{Erf}[x] \right) P_0 \\ &+ 21e^{x^2}x \left(3e^{2x^2}\pi(225 - 100x^2 + 12x^4)\text{Erf}[x]^2 \right) P_0, \end{aligned} \quad (41)$$

$$\begin{aligned} N_{P_{\delta\delta}P_2} &= 24e^{x^2}x^3 \left(2x^2(-210 + x^2 + 2x^4) + e^{x^2}\sqrt{\pi}x(420 - 37x^2 + 68x^4 + 4x^6)\text{Erf}[x] \right) P_2 \\ &+ 24e^{x^2}x^3 \left(3e^{2x^2}\pi(-35 + 6x^2)\text{Erf}[x]^2 \right) P_2, \end{aligned} \quad (42)$$

$$N_{P_{\delta\delta}P_4} = 32e^{x^2}x^5 \left(4x^2(3 - x^2) - 2e^{x^2}\sqrt{\pi}x(6 - x^2 + 2x^4)\text{Erf}[x] + 3e^{2x^2}\pi\text{Erf}[x]^2 \right) P_4, \quad (43)$$

$$\begin{aligned} N_{AP_0} &= -84e^{x^2}x^3 \left(4x^2(225 + 60x^2 + 6x^4 + 4x^6) + 4e^{x^2}\sqrt{\pi}x(-225 + 90x^2 + 29x^4 + 8x^6 + 4x^8)\text{Erf}[x] \right) P_0 \\ &- 84e^{x^2}x^3 \left(3e^{2x^2}\pi(75 - 80x^2 + 12x^4)\text{Erf}[x]^2 \right) P_0, \end{aligned} \quad (44)$$

$$\begin{aligned} N_{AP_2} &= -24e^{x^2}x^5 \left(2x^2(63 + 48x^2 + 4x^4) + e^{x^2}\sqrt{\pi}x(609 + 298x^2 + 100x^4 + 8x^6)\text{Erf}[x] \right) P_2 \\ &+ 24e^{x^2}x^5 \left(24e^{2x^2}\pi(14 - 3x^2)\text{Erf}[x]^2 \right) P_2, \end{aligned} \quad (45)$$

$$N_{AP_4} = 64e^{x^2}x^7 \left(6x^2 + 4x^4 + e^{x^2}\sqrt{\pi}x(9 + 8x^2 + 4x^4)\text{Erf}[x] - 6e^{2x^2}\pi\text{Erf}[x]^2 \right) P_4, \quad (46)$$

$$\begin{aligned} N_{BP_0} &= -84e^{x^2}x^5 \left(4x^2(45 + 4x^4) + 4e^{x^2}\sqrt{\pi}x(-45 + 30x^2 + 2x^4 + 4x^6)\text{Erf}[x] \right) P_0 \\ &- 84e^{x^2}x^5 \left(3e^{2x^2}\pi(15 - 20x^2 + 4x^4)\text{Erf}[x]^2 \right) P_0, \end{aligned} \quad (47)$$

$$N_{BP_2} = -48e^{x^2}x^7 \left(42x^2 + 4x^4 + e^{x^2}\sqrt{\pi}x(63 + 44x^2 + 4x^4)\text{Erf}[x] - 6e^{2x^2}\pi(7 - 2x^2)\text{Erf}[x]^2 \right) P_2, \quad (48)$$

$$N_{BP_4} = 128e^{x^2}x^9 \left(2x^2 + e^{x^2}\sqrt{\pi}x(1 + 2x^2)\text{Erf}[x] - e^{2x^2}\pi\text{Erf}[x]^2 \right) P_4, \quad (49)$$

$$\begin{aligned} D_P &= 315 \left(4x^3(21 + 2x^2) - 4e^{x^2}\sqrt{\pi}x^2(9 - 28x^2)\text{Erf}[x] - e^{2x^2}\pi x(27 + 58x^2 - 20x^4 + 8x^6)\text{Erf}[x]^2 \right) \\ &+ 315 \left(12e^{3x^2}\pi^{3/2}\text{Erf}[x]^3 \right) \end{aligned} \quad (50)$$

Thus, one can obtain the ratios of multipoles of Eqs.(36) and (37) by using the observed values of multipoles in the reference [1]. We compare these ratios of multipoles with those of liner theory. We constrain our analysis only for the North Galactic Cap (NGC) with including hexadecapole data in order to reduce the systematics. There are nine k values in DR12 for the hexadecapole.

First, we show the consistency of BOSS DR12 results for the growth index, f for three redshift bins. One can use the theoretical expectation values of $\sigma_8(z) = (D_1(z)/D_1(z_0))\sigma_8(z_0)$ to obtain $f(z)$ from the observed $f(z)\sigma_8(z)$ values. We show this in Fig.1. The solid line represents the theoretical values of $f(z)$ based on the fiducial model, Λ CDM with $\Omega_{m0} = 0.31$ and $\sigma_8(z_0) = 0.8$. The vertical dashed lines depict the DR12 data at three redshifts, $z = 0.38, 0.51$, and 0.61 . $f(z)$ value at $z_{\text{eff}} = 0.61$ deviates from the theoretical one by about 1.4σ as indicated in the reference.

Now we investigate the ratios of multipoles at three different redshifts using the observed values of multipoles. At the effective redshift $z_1 = 0.38$, one can obtain the ratio of quadrupole (hexadecapole) to monopole, $R_2(R_4)$ from the given DR12 data by using the analytic formulae Eqs.(36) and (37). The left panel of Fig.2 depicts the both linear and quasi-linear R_2 s. The dark shaded regions are the theoretical prediction of the ratio of the quadrupole to the monopole for the Kaiser limit, R_2^{Kai} given by Eq.(10) with $1\text{-}\sigma$ error. Observation provides both the value of $f(z_1)\sigma_8(z_1)$ and that of $b(z_1)\sigma_8(z_1)$ with the present fiducial value of $\sigma_8(z_0) = 0.8$. Thus, one can obtain $f(z_1)$ and $b(z_1)$ within $1\text{-}\sigma$ error to obtain the corresponding $R_2^{\text{Kai}}(z_1)$. These are k independent values ranged from 0.406 to 0.469. The bright shaded lines are the $1\text{-}\sigma$ regions of the linear theory with the FoG effect represented by R_2^{lin} . By including the FoG, one obtains the k -dependence of R_2 as given in Eq.(21). For large scale, $k < 0.03h/\text{Mpc}$, R_2^{lin} is almost same as R_2^{Kai} and it starts to show the small scale damping effect from $k > 0.03h/\text{Mpc}$. At $k = 0.095h/\text{Mpc}$, the values of R_2^{lin} is ranged from 0.285 to 0.369. The vertical dashed lines are $1\text{-}\sigma$ values of R_2 obtained from DR12

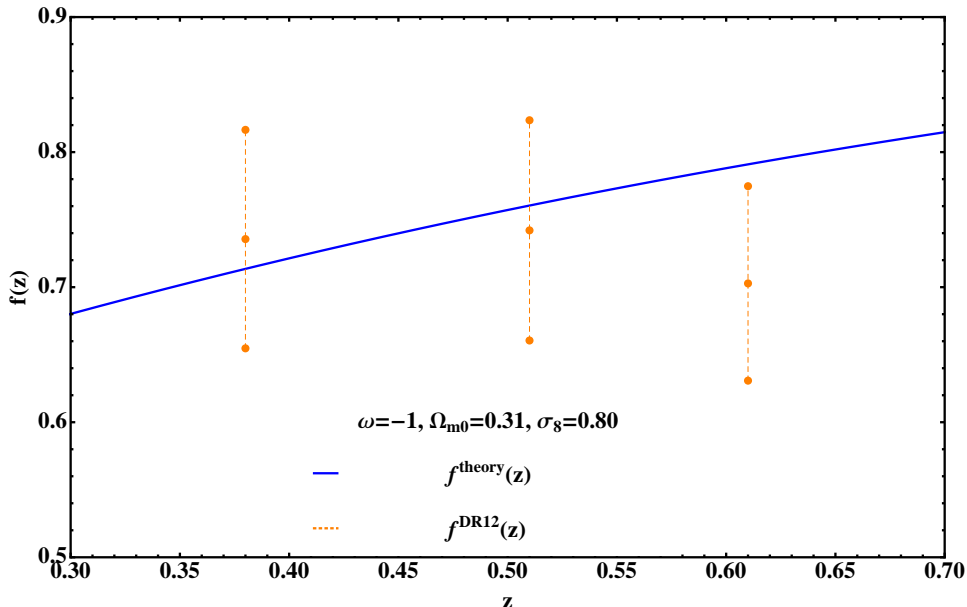


FIG. 1: The evolution of the growth index, $f(z)$. The solid line depicts the theoretical values of $f(z)$ based on the fiducial model, Λ CDM with $\Omega_{m0} = 0.31$ and $\sigma_8(z_0) = 0.80$. The dashed lines represent the DR12 data at three different redshifts.

multipoles. All of the observed R_2 values except the largest scale at $k = 0.016$ h/Mpc are consistent with the linear theory prediction for eight k bins from 0.025 h/Mpc to 0.095 h/Mpc. However, the current observation error is too large to investigate the any deviation of quasi-linear results from that of the linear theory. We also show the theoretical predictions and observation for the ratio of the hexadecapole to monopole, R_4 in the right panel of Fig.2. The dark shaded regions are the $1-\sigma$ theoretical prediction of R_4 for the Kaiser limit, R_4^{Kai} given by Eq.(11). These values range from 0.021 to 0.027 for the observed values of f and b at $z = 0.38$. The bright shaded lines are the $1-\sigma$ regions of the linear theory with the FoG effect, R_4^{lin} . This values range from 0.000 to 0.007 at $k = 0.095$ h/Mpc. However, the observed values of R_4^{Quas} are sparse and the most of them are deviated from the prediction of the linear theory as shown in the right panel of Fig.2.

We repeat the same analysis for R_2 and R_4 at the effective redshift $z_2 = 0.51$ as that of z_1 . The left panel of Fig.3 depicts the R_2 s. The Kaiser limit prediction of R_2 ranges from 0.394 to 0.455 which represented by the dark shaded lines. The bright shaded lines are the $1-\sigma$ regions of the linear theory with the FoG effect, R_2^{lin} . Again both R_2^{lin} and R_2^{Kai} are consistent with each other up to $k < 0.04$ h/Mpc. At $k = 0.095$ h/Mpc, the values of R_2^{lin} is ranged from 0.300 to 0.379 within $1-\sigma$. The vertical dashed lines are $1-\sigma$ values of R_2 obtained from DR12 multipoles. All of the observed R_2 values are consistent with both the linear theory prediction and that of the Kaiser limit except for two largest scales at $k = 0.016$ and 0.026 h/Mpc. We show the R_4 in the right panel of Fig.3. The dark shaded regions are R_4^{Kai} . The values of R_4^{Kai} range from 0.019 to 0.025 for the observed values of f and b at $z = 0.51$. The bright shaded lines are the $1-\sigma$ regions of R_4^{lin} ranged from 0.003 to 0.010 at $k = 0.095$ h/Mpc. However, the most of the observed values of R_4^{Quas} are deviated from the linear prediction as shown in the right panel of Fig.3.

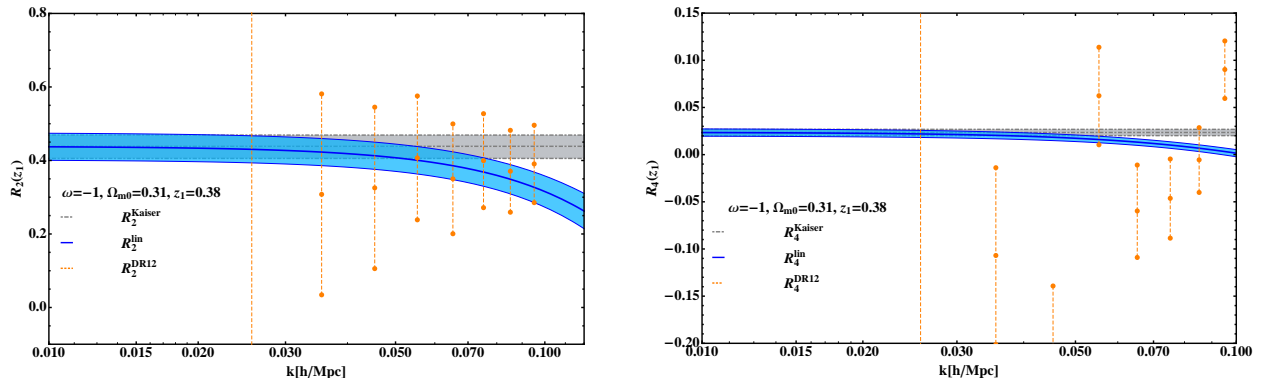


FIG. 2: The values of R_2 and R_4 at $z = 0.38$. a) The ratio of quadrupole to monopole, R_2 . The dark shaded lines are the 1- σ regions of the Kaiser limit. The bright shaded lines are the 1- σ regions of the linear theory. The vertical dashed lines indicate the 1- σ results of the DR12. b) The ratio of hexadecapole to monopole, R_4 with the same notation as in the left panel.

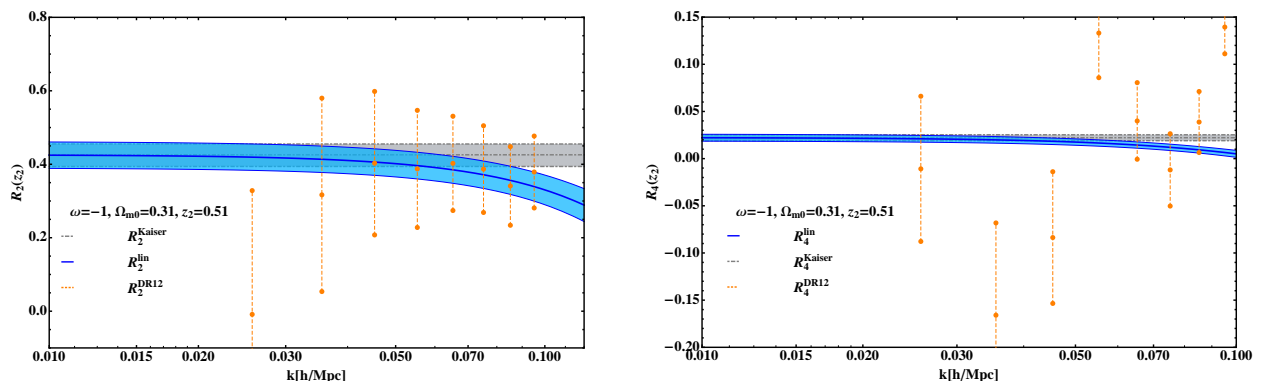


FIG. 3: The values of R_2 and R_4 at $z = 0.51$. a) R_2 with the same notations as those of Fig.2. b) R_4 .

R_2 and R_4 at the effective redshift $z_3 = 0.61$ are shown in Fig.4. The left panel of Fig.4 represents R_2 s at this epoch. The results show the consistency between the theory and the observation. The values of R_4 seems to be rather consistent with each other. However, this might be due to the inconsistency of the growth index, $f(z)$. This fact is shown in the right panel of Fig.4.

IV. CONCLUSIONS

We provide the analytic formulae for the multipoles and their ratio when one includes the Finger of God effect damping factor in the galaxy power spectrum. One can recover the galaxy power spectrum from the observed values of multipoles. We investigate the consistency of current DR12 multipoles data by comparing both theoretical and observational values of their ratio. The ratio of

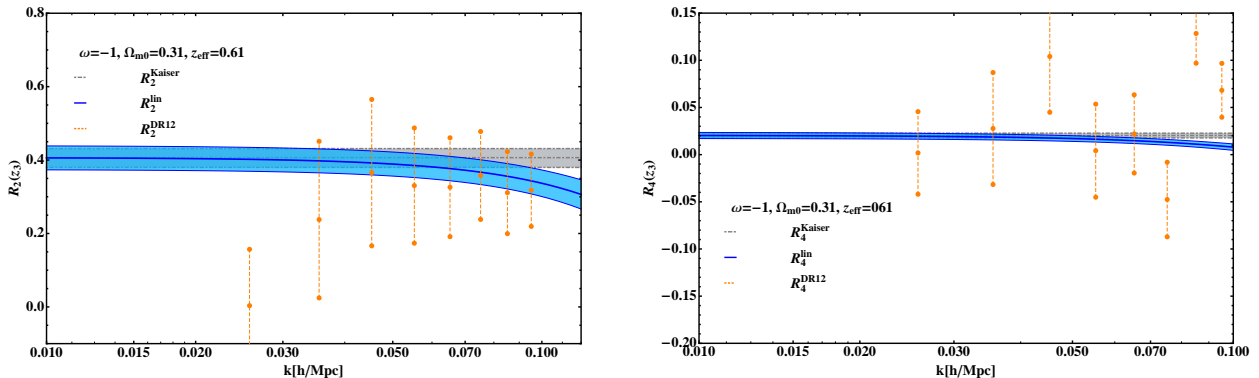


FIG. 4: The values of R_2 and R_4 at $z = 0.61$. a) R_2 . b) R_4 .

the quadrupole to the monopole is consistent with the prediction of the linear theory even though the current observational error cannot show the Finger of God effect. However, the ratio of the hexadecapole to the monopole is inconsistent with linear theory prediction even at large scales. Thus, the current observation of power spectrum multipoles is premature to be used to investigate the recovering power spectrum.

V. ACKNOWLEDGEMENTS

SL is supported by the Basic Science Research Program through the National Research Foundation of Korea (NRF) funded by the Ministry of Science, ICT and Future Planning (Grant No. NRF-2015R1A2A2A01004532). SL also thanks the department of physics at Sungkyunkwan University for their hospitality and support during the completion of this work.

VI. APPENDIX

In the appendix, we provide the analytic forms of multipoles and the their ratio when one uses the Lorentzian FoG factors given in Eqs.(15) and (16).

Multipoles of the linear power spectrum with the Lorentzian FoG factor given in Eq.(15) are given by

$$\frac{P_0^{(\text{lin})}}{P_{\delta\delta}^{(\text{lin})}} = \frac{fx(6x^2 + f(-3 + x^2)) + 3(f - x^2)^2 \text{ArcTan}[x]}{3x^5} \quad (\text{A.1})$$

$$\frac{P_2^{(\text{lin})}}{P_{\delta\delta}^{(\text{lin})}} = \frac{(-90fx^3 + 45x^5 + f^2x(45 + 4x^4) - 15(f - x^2)^2(3 + x^2) \text{ArcTan}[x])}{6x^7} \quad (\text{A.2})$$

$$\frac{P_4^{(\text{lin})}}{P_{\delta\delta}^{(\text{lin})}} = \frac{3(f - x^2)^2(-5x(21 + 11x^2) + 3(35 + 30x^2 + 3x^4) \text{ArcTan}[x])}{8x^9}, \quad (\text{A.3})$$

where $\text{ArcTan}[x]$ is the inverse tangent function of x . From Eqs.(A.1)-(A.3), one obtain the multi-poles ratios P_2/P_0 , P_4/P_0

$$\frac{P_2^{(\text{lin})}}{P_0^{(\text{lin})}} = \frac{-90fx^3 + 45x^5 + f^2x(45 + 4x^4) - 15(f - x^2)^2(3 + x^2) \text{ArcTan}[x]}{2x^2(fx(6x^2 + f(-3 + x^2)) + 3(f - x^2)^2 \text{ArcTan}[x])} \quad (\text{A.4})$$

$$\frac{P_4^{(\text{lin})}}{P_0^{(\text{lin})}} = \frac{9(f - x^2)^2(-5x(21 + 11x^2) + 3(35 + 30x^2 + 3x^4) \text{ArcTan}[x])}{8x^4(fx(6x^2 + f(-3 + x^2)) + 3(f - x^2)^2 \text{ArcTan}[x])} \quad (\text{A.5})$$

B. Conventional Lorentzian FoG

From the conventional Lorentzian FoG factor given in Eq.(16), multipoles of the linear power spectrum are obtained as

$$\frac{P_0^{(\text{lin})}}{P_{\delta\delta}^{(\text{lin})}} = \frac{2fx(6x^2 + f(-6 + x^2)) + 6c(2f - x^2)^2 \text{ArcTan}[cx]}{3x^5} \quad (\text{B.1})$$

$$\frac{P_2^{(\text{lin})}}{P_{\delta\delta}^{(\text{lin})}} = \frac{180fx(f - x^2) + x^5(45 + 4f^2) - 15c(6 + x^2)(-2f + x^2)^2 \text{ArcTan}[cx]}{3x^7} \quad (\text{B.2})$$

$$\frac{P_4^{(\text{lin})}}{P_{\delta\delta}^{(\text{lin})}} = \frac{-15x(-2f + x^2)^2(42 + 11x^2) + 9c(-2f + x^2)^2(140 + 60x^2 + 3x^4) \text{ArcTan}[cx]}{4x^9} \quad (\text{B.3})$$

where $c = \sqrt{0.5}$. From Eqs.(A.1)-(A.3), one obtains the multipoles ratios P_2/P_0 , P_4/P_0

$$\frac{P_2^{(\text{lin})}}{P_0^{(\text{lin})}} = \frac{-180fx^3 + 45x^5 + 4f^2x(45 + x^4) - 15c(6 + x^2)(-2f + x^2)^2 \text{ArcTan}[cx]}{2x^2(fx(6x^2 + f(-6 + x^2)) + 3c(-2f + x^2)^2 \text{ArcTan}[cx])} \quad (\text{B.4})$$

$$\frac{P_4^{(\text{lin})}}{P_0^{(\text{lin})}} = \frac{9(-2f + x^2)^2(-5x(42 + 11x^2) + 3c(140 + 60x^2 + 3x^4) \text{ArcTan}[cx])}{8x^4(fx(6x^2 + f(-6 + x^2)) + 3c(-2f + x^2)^2 \text{ArcTan}[cx])} \quad (\text{B.5})$$

-
- [1] F. Beutler, *et. al.*, [arXiv:1607.03150].
 - [2] A. Taruya, T. Nishimichi, and S. Saito, *Phys. Rev. D* **82**, 063522 (2010) [arXiv:astro-ph/1006.0699].
 - [3] R. Scoccimarro, *Phys. Rev. D* **70**, 083007 (2004) [arXiv:astro-ph/0407214].
 - [4] J. C. Jackson, *Mon. Not. R. Astr. Soc.* **156**, 1 (1972).
 - [5] J. A. Peacock and S. J. Dodds, *Mon. Not. R. Astr. Soc.* **280**, L19 (1996) [arXiv:astro-ph/9603031].
 - [6] N. Kaiser, *Mon. Not. R. Astr. Soc.* **227**, 1 (1987).
 - [7] C. Alcock and B. Paczynski, *Nature* **281**, 358 (1979).
 - [8] W. E. Ballinger, J. A. Peacock, and A. F. Heavens, *Mon. Not. R. Astr. Soc.* **282**, 877 (1996) [arXiv:astro-ph/9605017].
 - [9] L. Anderson, *et. al.*, *Mon. Not. R. Astr. Soc.* **427**, 3435 (2012) [arXiv:1203.6594].
 - [10] L. Samushia, *et. al.*, *Mon. Not. R. Astr. Soc.* **429**, 1514 (2013) [arXiv:1206.5309].
 - [11] K. Yamamoto, B. A. Bassett, and H. Nishioka, *Phys. Rev. Lett.* **94**, 051301 (2005) [arXiv:astro-ph/0409207].
 - [12] F. Beutler, *et.al.*, *Mon. Not. Roy. Astron. Soc.* **443**, 1065 (2014) [arXiv:1312.4611].
 - [13] P. A. R. Ade, *et.al.* [Planck Collaboration], [arXiv:1502.01589].
 - [14] B. A. Reid and M. White, *Mon. Not. R. Astr. Soc.* **417**, 1913 (2011) [arXiv:1105.4165].
 - [15] J. A. Peacock, *Mon. Not. R. Astr. Soc.* **258**, 581 (1992)
 - [16] M. Davis and P. J. E. Peebles, *Astro. Phys. J* **267**, 465 (1983).
 - [17] S. Lee, C. Park, and S. G. Biern, *Phys. Lett. B* **736**, 403 (2014) [arXiv:1407.7325].
 - [18] M. Tegmark, A. J. S. Hamilton, and Y. Xu, *Mon. Not. Roy. Astron. Soc.* **335**, 887 (2002) [arXiv:astro-ph/0111575].
 - [19] M. Tegmark and *et.al.*, *Astro. Phys. J* **606**, 702 (2004) [arXiv:astro-ph/0310725].